JOURNAL OF BACTERIOLOGY, Jan. 1991, p. 751–756
0021-9193/91/020751-06$02.00/0

Vol. 173, No. 2

Direct Proof of a "More-Than-Single-Layered" Peptidoglycan Architecture of *Escherichia coli* W7: a Neutron Small-Angle Scattering Study†

H. LABISCHINSKI,[1]* E. W. GOODELL,[2] A. GOODELL,[2] AND M. L. HOCHBERG[2]

Robert Koch Institute of the Federal Health Office, Nordufer 20, D-1000 Berlin 65, Federal Republic of Germany,[1] and SUNY Institute of Technology, Utica, New York, 13504-3050[2]

Received 22 June 1990/Accepted 2 November 1990

A neutron small-angle scattering study was performed to determine the thickness and the scattering density profile of isolated peptidoglycan sacculi of *Escherichia coli* W7 in aqueous suspension (D_2O). The maximum thickness (7 ± 0.5 nm) of the sacculus from the exponential-phase cells was large enough to suggest the existence of a more-than-single-layered architecture. The experimental density profile across the thickness of the sacculus did not allow an unambiguous differentiation between a single-layered architecture characterized by completely extended peptide side chains projecting from the sugar strands or, alternatively, a partially triple layered structure. To resolve this ambiguity, sacculi were labeled with deuterated wall peptides. Comparison of the two experimental profiles indicated that the sacculus is more than single layered across its surface, with about 75 to 80% of its surface single layered and 20 to 25% triple layered.

One of the most characteristic differences between gram-positive and gram-negative bacteria is the existence of a thick, multilayered peptidoglycan sacculus in the former type of bacteria and a thin peptidoglycan network in the latter. The difference in architecture of this well-defined cell wall component seems to be the major reason for the different staining behaviors between the two types of bacteria (2). The sacculi of both types of bacteria are made from peptidoglycan (murein), a polymer of relatively short glycan strands (average length in *Escherichia coli* of about 25 nm) that are cross-linked by short peptide bridges (for a review with emphasis on *E. coli*, see reference 18). On the basis of conventional transmission electron microscopic data showing a peptidoglycan layer of only about 3-nm thickness (8, 24), a single-layered sacculus was generally assumed to form the basic architecture for gram-negative bacteria. However, the amount of peptidoglycan per cell seems sufficient to form a double or even triple layer (6). Therefore, the basic structure of the sacculus, whether single layered or multilayered, as well as the mode of cell wall enlargement and formation during growth and division remained unresolved. The insertion type of model for incorporation of nascent murein suggests the existence of a single-layered peptidoglycan (6, 19, 25), while the inside-to-outside growth model is compatible with a triple-layered architecture (13, 28).

The exact architecture of gram-negative peptidoglycan sacculi is difficult to determine because there are no direct methods of observing or measuring a structure in the colloidal range of 1 to 10 nm under native conditions (e.g., full hydration of the sacculus). Research methods which provided indirect evidence for a multilayered arrangement of the sacculus include electron microscope observations using new preparation techniques, such as low-temperature embedding and freeze substitution (17) or special staining techniques (23), as well as studies using sophisticated high-performance liquid chromatography techniques (12, 13) combined with theoretical and model building studies (22, 21). One method that has been extensively used for the study of systems with colloidal dimensions, including many biologically important macromolecules and assemblies at fully hydrated conditions, is the small-angle scattering technique in solution (11). An important aspect of this technique is observed with anisotropic particles (one or two dimensions larger than the other dimension[s], i.e., rodlike or lamellalike particles). The scattering contribution due to the short axis (axes) of the particle can be easily separated from the total scattering, although the particles are in a random orientation in solution. Thus, for lamellalike particles such as sacculi, the distribution of material across their thickness axes, as well as their average surface thickness, can be studied. Interestingly, this technique has already been applied to gram-positive sacculi (32). In this instance, however, the gram-positive multilayered arrangement was used only as a test system to study the applicability of a magnetically based orientation setup.

Either neutrons or X rays can be used as the primary exciting beam with the small-angle scattering technique. One specific advantage in using a neutron beam is that molecules containing hydrogen atoms can be distinguished from those which contain the isotope of hydrogen, deuterium (11). Hydrogen atoms have a negative scattering length (-0.372×10^{-12} cm), i.e., they tend to diminish the amount of scattered intensity, while deuterium is strongly positive ($+0.67 \times 10^{-12}$ cm). Thus, somewhat similar to radiolabeling techniques, scattering label techniques can be performed by labeling molecules with deuterium (31). Deuterated peptides (isolated from *E. coli* grown on D_2O) can be used to label the sacculus since they are taken up and incorporated into the murein without being degraded (14). We hypothesized that this would allow us to measure the thickness and scattering density distribution across the thickness of the sacculus as well as to localize the position of the peptide component within the sacculus. In addition, the deuterium labeling

* Corresponding author.

†This paper is dedicated to the late E. W. Goodell, who has provided a substantial increase in knowledge of the structure of *E. coli* sacculi. His expertise will be missed by his colleagues and friends.

technique might also be useful for monitoring the fate of newly inserted peptidoglycan units.

The experiments described in this report provide the first information on the structure of the *E. coli* sacculus obtained by using a small-angle neutron scattering technique. A comparison of the hydrogenated and deuterated experimental profiles indicated that the sacculus was neither single layered nor multilayered across its complete surface but more than single layered, with about 75 to 80% of its surface a monolayer and 20 to 25% a triple layer of peptidoglycan.

MATERIALS AND METHODS

Bacterial strains and culture conditions. *E. coli* W7 (Dap^- Lys^-) was grown in minimal C medium (16) supplemented with glucose (0.2%), $MgSO_4$ (0.25 mg/ml), and all essential L-amino acids except cysteine (40 μg/ml each). The nondeuterated cells were grown in the minimal C medium (including essential amino acids) with diaminopimelic acid (20 μg/ml). The cells containing deuterated murein peptides were grown for approximately six generations in a medium containing tri- and tetrapeptides instead of diaminopimelic acid as previously described (15). The tri- and tetrapeptides contained almost 100% deuterium, and the peptides in the sacculi isolated from cells grown for six generations in D-peptides were over 90% labeled with deuterium. Both cultures were grown to an optical density at 578 nm of 0.5.

Preparation of deuterated murein peptides. Murein membrane fractions of *E. coli* grown in D_2O were a kind gift of H. Heumann and H. Lederer, Max-Planck-Institut für Biochemie, Munich, Federal Republic of Germany. All murein peptides used for labeling experiments were 100% deuterated, since all medium constituents for growing the bacteria used for peptide isolation were in a deuterated form. However, some exchange of hydrogen for deuterium took place during isolation of the peptides and during labeling experiments, since these procedures were all performed in a normal water environment. Murein peptides were purified from membrane fractions as described previously (14). Membrane fractions were boiled in 4% sodium dodecyl sulfate (SDS) for 15 min, washed in distilled water, and centrifuged (100,000 × *g*, 30 min) five times. The isolated murein was digested with human amidase, and the tri- and tetrapeptides were isolated by passing the digested products over a Fractogel TSK-HW-40-S column (2.5 by 60 cm; E. Merck AG, Darmstadt, Federal Republic of Germany; elution buffer was 20 mM ammonium acetate in 25% ethanol) (14, 27).

Isolation and preparation of sacculi. The growth of bacteria (labeled with deuterated peptides or unlabeled) was stopped by rapid transfer of the culture into a flask containing ice. The cells were pelleted, resuspended in cold distilled H_2O, transferred into boiling 4% SDS for 15 min, washed with distilled water, and centrifuged (100,000 × *g*, 30 min) five times. α-1,4-Glycan, which had been found in cell wall preparations of *E. coli* W7 (12), and lipoprotein were digested successively by incubation with α-amylase (Sigma) at 100 μg/ml for 2 h at 37°C and trypsin (Sigma) at 100 μg/ml for 1 h in 10 mM Tris hydrochloride–10 mM NaCl (pH 7.4). The enzymes were inactivated by boiling in 1% SDS for 10 min, and the suspension was centrifuged three times (100,000 × *g*, 30 min). The digestion procedure with amylase and trypsin was repeated to ensure complete digestion of all nonmurein carbohydrates and proteins. The cell wall preparation was resuspended in D_2O and centrifuged three times (100,000 × *g*, 30 min) to exchange the H_2O for D_2O. The final pellet was resuspended in approximately 1 ml of D_2O per 1.5 mg (dry weight) of sacculi for a final sample volume of 200 to 250 μl. The supernatant of the final wash was retained and used as a measurement for background in the neutron scattering studies.

Neutron scattering data collection and evaluation. Small-angle neutron scattering experiments were performed with the H 9-B small-angle scattering instrument (29) of the high-flux beam research reactor at the Brookhaven National Laboratory, Upton, N.Y. Samples were measured in quartz flasks (path length, 3 mm; approximately 200 μl per sample) at room temperature. Sample scattering curves were corrected for contributions of buffer, empty cell, and background counts. The radially averaged scattering curves (angular range $Q = 0.2$ to 3.3 nm^{-1}; $Q = 4\pi \cdot \sin\Theta/\lambda$; 2Θ = full scattering angle; λ = wavelength) were deconvoluted with the wavelength and primary beam profiles by using the indirect Fourier transformation program ITP of Glatter (9, 10). The program was also applied to calculate the thickness distance distribution function $\gamma(r)$, which describes the probability of finding a given distance r between any two positions across the thickness of a sacculus, weighted by the scattering-length densities at these positions. From the second moment of this function, the corresponding thickness radius of gyration was calculated and the maximum length across the sacculus was taken from the distance r_{max}, where the distance distribution function reached the value 0.

RESULTS

Thickness determination by neutron scattering on nondeuterated sacculi. Since the neutron scattering technique can only distinguish between the scattering density of the macromolecule and the solvent system, this contrast is of primary importance. The scattering density of each component can be estimated from the sum of the tabulated scattering-length contributions of the individual atoms forming the respective component divided by the volume occupied by these atoms (31). In this way, the scattering-length densities of the peptide and sugar portions were estimated to be approximately 2.5 in the usual units of 10^{10} cm^{-2}, while those of H_2O and D_2O are −0.56 and 6.34, respectively (31). Since the contrast of the sacculi suspended in either H_2O or D_2O was nearly identical, but H_2O produces strong incoherent background of scattering (31), we decided to perform all neutron scattering experiments in D_2O. A gel-like, stable suspension of sacculi was used for all samples (ca. 1.5 mg of sacculi in 1.0 ml of D_2O) to prevent sedimentation of the sacculi during scattering experiments.

Figure 1a shows the experimental scattering curve, i.e., logarithm of intensity I of the scattered beam versus the scattering angular variable Q ($Q = 4\pi \cdot \sin\Theta/\lambda$; Θ = half of the scattering angle; λ = wavelength of the neutrons), and Figure 1b shows the thickness distance distribution function $\gamma(r)$ calculated from Fig. 1a by the method of indirect Fourier transformation (9, 10). Since the distance distribution function represents the probability of finding any distance r to occur within the thickness of the sacculus, it has its largest values when r is small (the probability of finding a small distance to occur within the sacculus is high) and vanishes at the maximum diameter r_{max}, which can be measured from Fig. 1b as 7 ± 0.5 nm. It should be noted that this value represents the maximum thickness of the sacculus (as opposed to a mean value). The maximum thickness may be found only in some regions of the peptidoglycan network and not necessarily across the complete surface of the sacculus. In fact, if the sacculus had a constant density over its entire

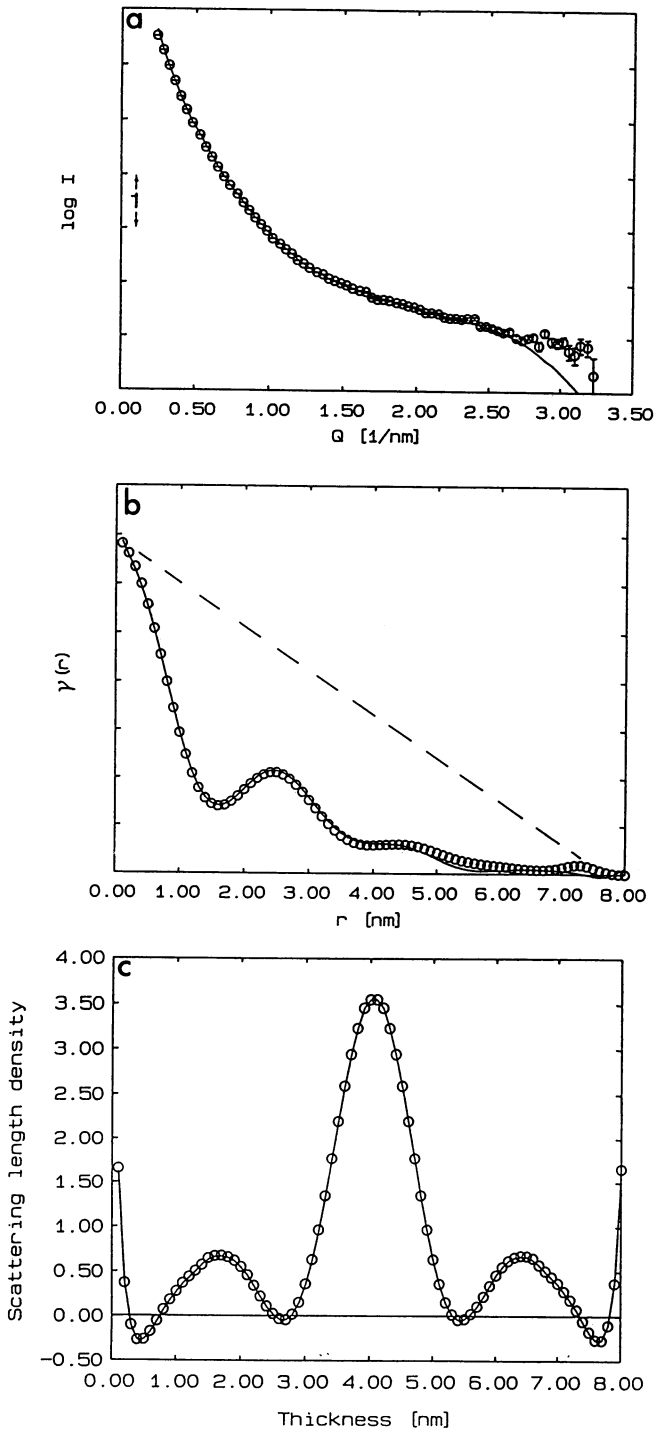

FIG. 1. Neutron small-angle scattering data on sacculi containing nondeuterated peptides. (a) Experimental neutron scattering data, log intensity versus the angular variable Q (○) and fitted intensity curve (——) obtained with the indirect Fourier transform technique (9, 10) used to calculate the thickness distance distribution function shown in panel b. The minor deviations between the experimental and fitted intensity curves at high Q values are probably due to small residual background scattering contributions and are of neglegible influence on the data shown in panels b and c. (b) Distance distribution function [$\gamma(r)$; arbitrary units] calculated from panel a, revealing a maximum sacculus thickness of 7 ± 0.5 nm and a substructure with ca. 2.5-nm periodicity. The dashed line indicates the distance distribution function for a structure with the same dimensions but uniform density distribution across the thickness. (c) Scattering density profile across the thickness of the *E. coli* sacculus calculated from the distance distribution function shown in panel b. For details, see text.

surface and could be approximated by a single box shape, the distance distribution function would reflect this by a linear decrease toward larger r values. This obviously was not the case (Fib. 1b). Instead, the quasiperiodical side maxima at ca. 2.5 and 5 nm demonstrated a variation in scattering density, with a 2.5-nm periodicity across the sacculus.

The thickness also can be determined from another important parameter, calculated from the scattering data and the $\gamma(r)$ function, namely, the radius of gyration R of the thickness. This physical quantity is completely analogous to the common radius of inertia well known from mechanics, not weighted by mass but by scattering density, according to the following formula:

$$R^2 = \frac{\int_0^\infty \gamma(r) \cdot r^2 \cdot dr}{2 \int_0^\infty \gamma(r) \cdot dr}$$

The radius of gyration was determined according to the above equation, with $R = 1.6 \pm 0.1$ nm. The proof for consistency of these calculations was determined according to the well-known Guinier approximation with $R = 1.5 \pm 0.1$ nm. From this value, an equivalent thickness of a structure could be calculated which has the same radius of gyration and a constant density across its thickness of about 5.0 to 5.5 nm ($= R \cdot \sqrt{12}$) (11). The discrepancy between this value and the experimental r_{max} of 7.0 nm indicated again that the real scattering density across the thickness of the sacculus was nonuniform but higher in its center. This is more easily observed when the distance distribution is deconvoluted into a profile corresponding to the direct scattering density variation across the thickness of the sacculus (Fig. 1c). However, while it is easy to calculate the distance distribution function for any density profile, it is not possible to obtain the density profile directly from the distance distribution function because of the well-known phase problem of X-ray and neutron scattering theory (11). We therefore used several centrosymmetric model profiles (e.g., box shaped, one to three Gaussian curves, etc.) to mimic the profiles for single-, double-, or triple-layered sacculi. These provided starting models for a subsequent least-square fit minimization using the Powell algorithm (26). The quantity minimized was the sum of squares of the deviations between the experimental and the model distance distribution functions. Independent of the various starting models, good approximations were obtained only when the final model converged to the profile shown in Fig. 1c. Thus, a model using a double-layered structure could not account for the course of the thickness distribution function with a threefold modulation as the experimental one (cf. Fig. 1b). Even when models corresponding to mixtures of double- and triple-layered

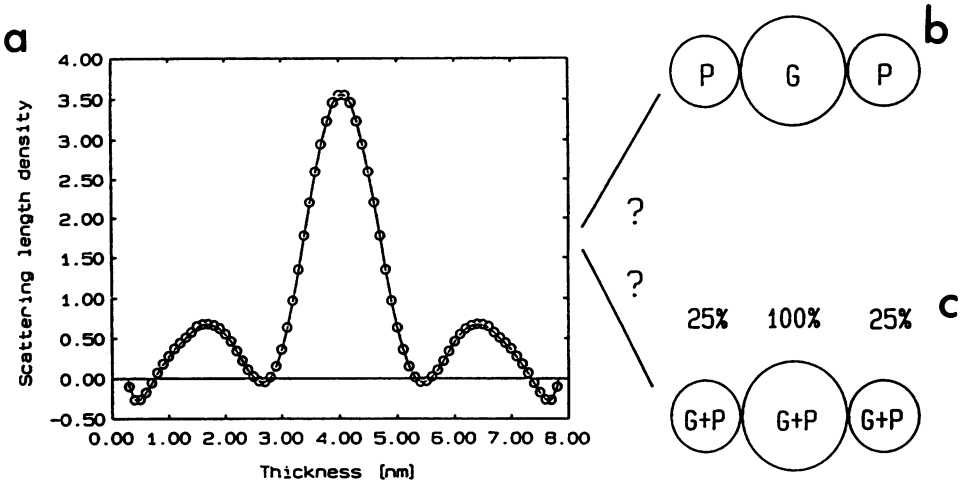

FIG. 2. Schematic representation of two possible peptidoglycan arrangements compatible with the experimental density profile across the thickness of the sacculus (a) of sacculi of *E. coli* W7 from the logarithmic phase of growth. (b) Single-layered model with central glycan chain (G) and extended peptide chain (P) substitution. (c) Partially triple layered model.

structures were used in the calculations, the starting model was changed by the minimization procedure to that shown in Fig. 1c. One should note that this optimized model also did not fully explain the experimental thickness distribution function at large r values (cf. the small deviations between the experimental and calculated functions at large r values in Fig. 1b). This might be due to the existence of a very small proportion of the sacculus surface containing more than three layers. It is important to note that other, noncentrosymmetrical profiles cannot be excluded by this procedure, since the thickness distribution function is always centrosymmetrical (i.e., if there is a distance, say, from layer 1 to layer 2, there is also the centrosymmetrical one from layer 2 to layer 1) (see Discussion).

The most striking feature of the density profile shown in Fig. 1c is the existence of a large central core of about 2.5 nm at the borders, wherein the density reaches the level of the solvent, surrounded by two regions again of approximately 2.5 nm thickness but with much less density. Two different structural interpretations could be consistent with this profile (Fig. 2). The larger-density peak in the middle of the sacculus could represent a central glycan strand, with the lower-density peaks representing the peptides which may project away from the sugar strands. A second interpretation also is possible, since the neutron scattering data represent an average over the entire sacculus. Some regions of the sacculus could contain only a single-layered structure while others could contain a triple-layered architecture, with a ratio of the two approximately 4 to 1.

Discrimination between single-layered or partially triple layered peptidoglycan by neutron scattering. To discriminate between the two structural models shown in Fig. 2, i.e., a single-layered peptidoglycan with extended peptide chains or a partially triple layered murein, the scattering experiment described above for sacculi containing only hydrogenated peptides was repeated by using the sacculi containing deuterated peptides. In D_2O suspension, the average scattering-length density of the deuterated peptide can be estimated at approximately 5.8 in units of 10^{-10} cm^{-2}. Thus, the contrast between deuterated peptides and D_2O suspension (density =

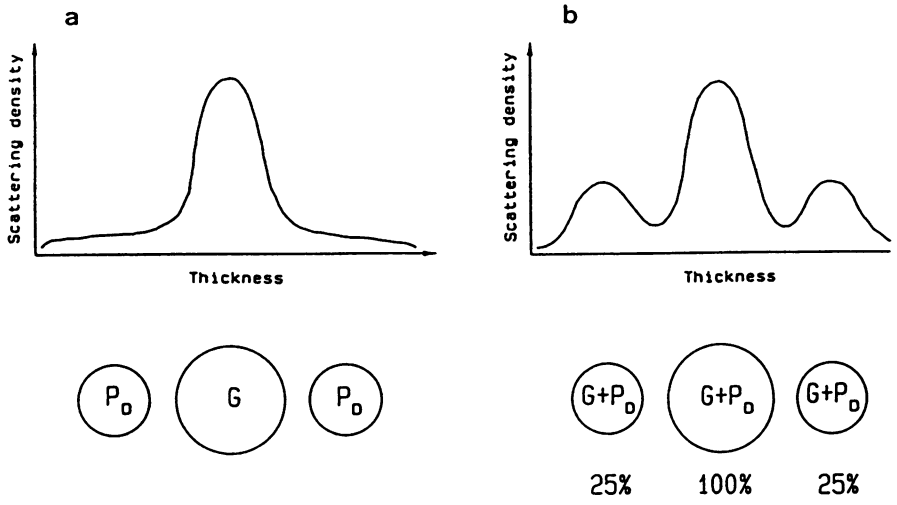

FIG. 3. Predicted influence of deuterated wall peptide on the neutron scattering density profile of *E. coli* peptidoglycan for the single-layered model (a) and for the partially triple layered model (b) (cf. Fig. 2). G, Glycan strand; P_D, deuterated peptide moiety.

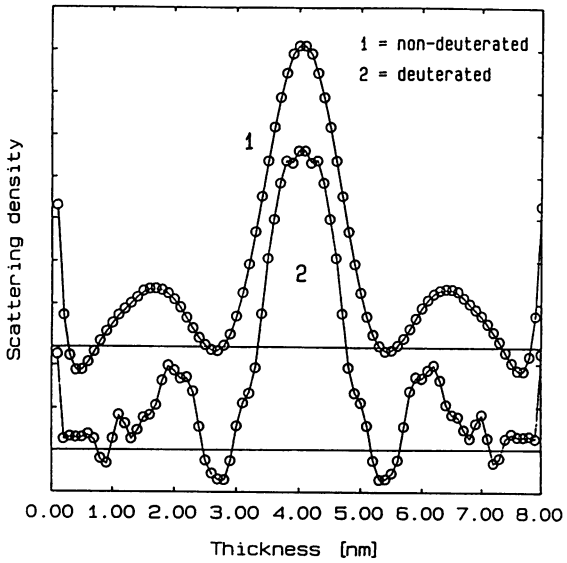

FIG. 4. Comparison between the neutron scattering-length density profiles of nondeuterated (1) and deuterated (2) sacculi of *E. coli* W7.

6.34×10^{-10} cm^{-2}) is nearly eliminated and much lower than that of the wall peptides containing hydrogen atoms (approximately 2.5×10^{-10} cm^{-2}).

As shown schematically in Fig. 3, the scattering density profiles expected for the two possible models would be quite different because the deuterated peptides cannot be more effectively detected by the neutron beam in a D_2O suspension. In the single-layered model with the peptide chains extended, the outermost peaks should be nearly as low as the solution level, since they contain only (deuterated) peptides. It should be noted that exchangeable hydrogen atoms of the peptides should also be deuterated, since all measurements were performed in D_2O. The profile compatible with the partially triple layered architecture, on the other hand, should be very similar to that shown in Fig. 1c and 2, since the peptides would be distributed over all three density peaks in the profile. The relative sizes of the three peaks should remain the same, since all of these peaks are being produced mainly by the glycan strands which contain only hydrogen atoms. Furthermore, the region between the three main density peaks should be diminished, since the peptides would be concentrated here. The experimental results shown in Fig. 4 compared with the profile from the sample containing only hydrogenated peptides clearly illustrate that the small peaks did not represent extended peptide chains. Therefore, these results provide clear evidence for the existence of a partially triple layered sacculus.

DISCUSSION

On the basis of thickness measurements and determination of the scattering density profiles across the thickness obtained by using *E. coli* W7 sacculi containing either hydrogen- or deuterium-labeled peptides, the neutron scattering data clearly provide evidence of the existence of a more-than-single-layered peptidoglycan in gram-negative bacteria. The murein sacculus of exponentially growing *E. coli* W7 contained a single-layered part (thickness of 2.5 nm) covering approximately 75 to 80% of its surface and a triple-layered part (thickness of about $3 \times 2.5 = 7.5$ nm) covering the remaining 20 to 25%. Interestingly, there was no evidence for the existence of a double-layered region or a more-than-triple-layered region. This result also shows that the experimental data were not influenced by artifacts due to aggregation, as has also been revealed by the results from preliminary X-ray experiments showing no influence of concentration on the scattering behavior up to the range of concentrations used for the neutron studies (data not shown). It also should be noted that the results were not influenced by the curvature of the sacculus or by any contacts of parts between two sacculi or by both sides of the same sacculus. This is because these conditions do not cause a coherent scattering contribution. However, it must be stated clearly that the density profiles shown in Fig. 1c, 2, and 4 represent only one possible variation (the centrosymmetrical one) of the common scheme: 75 to 80% single-layered and 20 to 25% triple-layered profile. This is because the scattering data result in a thickness distribution function, which by its very nature is always centrosymmetric and therefore cannot be used to differentiate between a centrosymmetrical or a nonsymmetrical architecture (e.g., both additional layers on the outside or inside of the single layer exclusively or any combination of these possibilities). Furthermore, the remaining small deviations at large r values between the experimental thickness distribution function and the one recalculated from the partially triple layered model might indicate the existence of a very small portion of the sacculus surface comprising even more than three layers.

It is interesting to compare the measured thickness of 7 ± 0.5 nm obtained under fully hydrated conditions in this study with those of electron microscopic data. Originally, the data from electron microscopic techniques indicated the thickness of the sacculus to be about 3 nm (8, 24). These lower values may have been caused by the dehydration of the relatively loose and strongly hydrated peptidoglycan. However, our results are in closer agreement with recent electron microscopic studies using new preparation techniques. Hobot et al. (17) reported results on isolated pure peptidoglycan as compatible with a somewhat fuzzy layer of 5 to 7 nm width by using low-temperature techniques, and Leduc et al. (23) reported a sacculus thickness of 6.6 ± 1.5 nm by using application of a special staining technique. Considering the difficulty in evaluating a width value from projection of sacculus sections much thicker than this width, the agreement with the neutron data seems to be very good.

If the distribution of the single- and triple-layered structures is assumed to occur in two clearly distinct regions of the sacculus, two attractive possibilities seem to exist. The first model would posit the existence of a single-layered peptidoglycan in the cylindrical wall region and a triple-layered peptidoglycan at the polar caps. The surface ratio of these two wall regions would roughly fit the experimentally observed proportions, and these two wall regions are synthesized independently under the control of different penicillin-binding proteins (1, 3, 7, 30). If the structure of the sacculus is similar to this model, then the intercalation-type model of growth proposed by Burman and Park (6) and Park (25) would be most plausible and would be in agreement with the predictions from conformational considerations which favored a partially multilayered structure in the polar cap region (21, 22). The alternative model would posit the existence of multilayered regions across some areas of the cylindrical surface (probably not centrosymmetrical), representing the growth zones in an inside-to-outside growth model as proposed by Glauner et al. (13). It appears possible that further neutron small-angle scattering studies would

answer important questions regarding the way in which nascent murein is added to the sacculus. We expect some of these answers from future pulse-chase studies using peptides labeled with deuterium and from analysis of sacculi from bacteria with large variations in the ratio of cylindrical to polar cap wall content. These studies would include the isolation of peptidoglycan from minicell preparations, which should predominantly contain polar cap material, and peptidoglycan from cells grown in the presence of nalidixic acid, which grow as filaments with a greatly enlarged proportion of cylindrical wall material.

The neutron scattering data, indicating the existence of a partially triple layered peptidoglycan and a thickness of 2.5 to 7 nm, also help us to understand the existence of oligomeric peptidoglycan subunits as trimers and tetramers at positions other than the chain ends. If only a single-layered sacculus exists, conformational considerations require that the oligopeptides be located at the ends of the glycan because of the helical conformation of the sugar chains (5, 20–22). The partial arrangement of the peptidoglycan in more than one plane, however, is easily consistent with the experimentelly observed existence of oligomeric units within the glycan chains (22), with most of the oligopeptides located between the layers. The neutron scattering profiles of the deuterated and hydrogenated peptide samples (Fig. 4) support the conclusion that the peptides are also located between glycan layers of the triple-layered regions of the sacculus and extending away from the glycan structural plane in the single-layered regions.

ACKNOWLEDGMENTS

We thank the administration and scientific personnel of the high-flux beam reactor facility and the Biology Department of the Brookhaven National Laboratory for allowing us to perform the neutron scattering experiments. We especially thank Dieter Schneider for his intense and stimulating support during the experiments. We are grateful to A. Brauer for most of the computer calculations and for skillful preparation of the figures and to E. Albrecht for typing of the manuscript.

This research was supported by Public Health Service grant AI25496-03 to M.L.H. from the National Institutes of Health.

REFERENCES

1. **Begg, K. J., and W. D. Donachie.** 1985. Cell shape and division in *Escherichia coli*: experiments with shape and division mutants. J. Bacteriol. **163**:615–622.
2. **Beveridge, T. J., and J. A. Davies.** 1983. Cellular responses of *Bacillus subtilis* and *Escherichia coli* to the Gram stain. J. Bacteriol **156**:846–858.
3. **Botta, G. A., and J. T. Park.** 1981. Evidence for involvement of penicillin-binding protein 3 in murein synthesis during septation but not during cell elongation. J. Bacteriol. **145**:338–340.
4. **Braun, V., H. Gnirke, U. Henning, and K. Rehn.** 1973. Model for the structure of the shape-maintaining layer of the *Escherichia coli* cell envelope. J. Bacteriol. **114**:1264–1270.
5. **Burge, R. E., A. G. Fowler, and D. A. Reaveley.** 1977. Structure of the peptidoglycan of bacterial cell walls. I. J. Mol. Biol. **177**:927–953.
6. **Burman, L. G., and J. T. Park.** 1984. Molecular model for elongation of the murein sacculus of *Escherichia coli*. Proc. Natl. Acad. Sci. USA **81**:1844–1848.
7. **De Jonge, B. L. M., F. B. Wientjes, J. Jurida, F. Driehuis, J. T. M . Wouters, and N. Nanninga.** 1989. Peptidoglycan synthesis during the cell cycle of *Escherichia coli*: composition and mode of insertion. J. Bacteriol. **171**:5783–5794.
8. **De Petris, S.** 1967. Ultrastructure of the cell wall of *Escherichia coli* and chemical nature of its constituent layers. J. Ultrastruct. Res. **19**:45–83.
9. **Glatter, O.** 1977. A new method for the evaluation of small angle scattering data. J. Appl. Crystallogr. **10**:415–421.
10. **Glatter, O.** 1980. Evaluation of small angle scattering data from lamellar and cylindrical particles by the indirect transformation method. J. Appl. Crystallogr. **13**:577–584.
11. **Glatter, O., and O. Kratky.** 1982. Small angle X-ray scattering. Academic Press, Inc., London.
12. **Glauner, B.** 1986. Das Murein von E. coli. Thesis. Universität Tübingen, Tübingen, Federal Republic of Germany.
13. **Glauner, B., J.-V. Höltje, and U. Schwarz.** 1988. The composition of the murein of *Escherichia coli*. J. Biol. Chem. **263**:10088–10095.
14. **Goodell, E. W.** 1985. Recycling of murein by *Escherichia coli*. J. Bacteriol. **163**:305–310.
15. **Goodell, E. W., and C. F. Higgins.** 1987. Uptake of cell wall peptides by *Salmonella typhimurium* and *Escherichia coli*. J. Bacteriol. **169**:3861–3865.
16. **Helmstetter, C. E., and S. Cooper.** 1986. DNA synthesis during cell division cycle of rapidly growing *Escherichia coli* B/r. J. Mol. Biol. **31**:507–518.
17. **Hobot, J. A., E. Carlemalm, W. Villinger, and E. Kellenberger.** 1984. Periplasmic gel: new concept resulting from the reinvestigation of bacterial cell envelope ultrastructure by new methods. J. Bacteriol. **160**:143–152.
18. **Höltje, J. V., and U. Schwarz.** 1985. Biosynthesis and growth of the murein sacculus, p. 77–119. *In* N. Nanninga (ed.), Molecular cytology of *Escherichia coli*. Academic Press, Inc., London.
19. **Koch, A. L., and I. D. J. Burdett.** 1984. The variable T model for gram-negative morphology. J. Gen. Microbiol. **130**:2325–2338.
20. **Labischinski, H., G. Barnickel, H. Bradaczek, and P. Giesbrecht.** 1979. On the secondary and tertiary structure of murein. Eur. J. Biochem. **95**:147–155.
21. **Labischinski, H., G. Barnickel, D. Naumann, and P. Keller.** 1985. Conformational and topical aspects of the three-dimensional architecture of bacterial peptidoglycan. Ann. Microbiol. (Inst. Pasteur) **136A**:45–50.
22. **Labischinski, H., and L. Johannsen.** 1986. On the relationships between conformational and biological properties of murein, p. 37–42. *In* P. H. Seidl and K. H. Schleifer (ed.), Biological properties of peptidoglycan. Walter de Gruyter, Berlin.
23. **Leduc, M., C. Frehel, E. Siegel, and J. van Heijenoort.** 1989. Multilayered distribution of peptidoglycan in the periplasmic space of *Escherichia coli*. J. Gen. Microbiol. **135**:1243–1254.
24. **Murray, R. G. E., P. Steed, and H. E. Elson.** 1965. The location of the mucopeptide in sections of the cell wall of *Escherichia coli* and other gram-negative bacteria. Can. J. Microbiol. **11**: 547–560.
25. **Park, J. T.** 1988. Does *Escherichia coli* use a left-handed murein endopeptidase and transpeptidase to assemble its sacculus?, p. 60–65. *In* P. Actor, L. Daneo-Moore, M. L. Higgins, M. R. J. Salton, and G. D. Shockman (ed.), Antibiotic inhibition of bacterial cell surface assembly and function. American Society for Microbiology, Washington, D.C.
26. **Powell, M. J. D.** 1964. An efficient method for finding the minimum of a function of several variables without calculating derivatives. Comput. J. **7**:155–162.
27. **Schwarz, U., A. Asmus, and H. Frank.** 1969. Autolytic enzymes and cell division of *Escherichia coli*. J. Mol. Biol. **41**:419–429.
28. **Schwarz, U., and B. Glauner.** 1988. Murein structure data and their relevance for the understanding of murein metabolism in *Escherichia coli*, p. 33–40. *In* P. Actor, L. Daneo-Moore, M. L. Higgins, M. R. J. Salton, and G. D. Shockman (ed.), Antibiotic inhibition of bacterial cell surface assembly and function. American Society for Microbiology, Washington, D.C.
29. **Shapiro, S., D. C. Rover, and H. Kuper.** 1983. HFBR handbook. Brookhaven National Laboratory, Upton, N.Y.
30. **Spratt, B. G.** 1975. Distinct penicillin-binding proteins involved in the division, elongation, and shape of *Escherichia coli* K 12. Proc. Natl. Acad. Sci. USA **72**:2999–3003.
31. **Stuhrmann, H. B., and A. Miller.** 1978. Small-angle scattering of biological structures. J. Appl. Crystallogr. **11**:325–345.
32. **Torbet, J., and M. Y. Norton.** 1982. Structure of the cell wall of *Staphylococcus aureus* studied with neutron scattering and magnetic birefringence. FEBS Lett. **147**:201–206.